LINEAR SCANNING METHOD BASED ON THE SAFT COARRAY

C. J. Martín[1], O. Martínez-Graullera[1], D. Romero[1], R. T. Higuti[2], and L. G. Ullate[1]

[1] Instituto de Automática Industrial - CSIC. Carretera de Campo Real, km 0.200. La Poveda. Arganda del Rey. Madrid. E-28500, Spain
[2] UNESP - Universidade Estadual Paulista. Dep. Electrical Engineering. Av. Brasil, 56, 15385-000, Ilha Solteira, SP, Brasil

ABSTRACT. This work presents a method to obtain B-scan images based on linear array scanning and 2R-SAFT. Using this technique some advantages are obtained: the ultrasonic system is very simple; it avoids the grating lobes formation, characteristic in conventional SAFT; and subaperture size and focussing lens (to compensate emission-reception) can be adapted dynamically to every image point. The proposed method has been experimentally tested in the inspection of CFRP samples.

Keywords: Linear array, ultrasonic NDE, SAFT
PACS: 43.35.Zc, 43.60.Fg.

INTRODUCTION

Linear array scanning is a common tool in ultrasonic NDE. These systems use electronic scanning and beamforming to activate a subaperture to capture/compose a single A-scan along the subaperture axis. This subaperture is swept along the length of the probe to create a cross-sectional profile without moving the transducer. Successive subapertures produce successive A-scans that are stacked to create a B-scan image.

Due to the fact that steering is not used, to increase the energy radiated in linear array probes the transducer elements usually are higher than conventional phased-array elements (a wavelength or more). Therefore, beamforming is limited to improve the A-scan quality in axis, with fixed focus on emission and dynamic focussing on reception. Futhermore, the distance between image lines is limited by the distance between elements in the aperture, and also the lateral resolution and the maximum subaperture size. Thus, although this technique is very simple and effective, it is unable to provide high quality images.

The superior performance of beamformed imaging for better evaluation of location and morphology of the defects, in front of traditional B-scan imaging, has been discussed [1]. Then, in order to adapt beamforming techniques to linear array imaging to increase the image quality, synthetic aperture imaging techniques (SAFT) [2] are proposed here. These techinques divide the image generation process in two stages: the first one is the acquisition stage, where all signals needed to compose the image are captured; and the second one is the beamforming stage, that can be dynamically tuned to the image requirements.

CP1211, *Review of Quantitative Nondestructive Evaluation Vol.29,*
edited by D. O. Thompson and D. E. Chimenti

The advantages that can be achieved are:

- Dynamically Focussing in emission and reception can be applied, increasing considerably the quality of the resulting images.
- The subaperture size can be dynamically adapted to the depth of focus, providing convenient resolution at all image points.

However, conventional SAFT introduce artifacs in the image that reduce the image quality. In this work we present a new synthetic aperture technique, known as 2R-SAFT [3], to eliminate these artifacts. Both conventional SAFT and 2R-SAFT are compared experimentally in CFRP components evaluation.

SAFT LINEAR IMAGING

If the level of energy radiated by one element is enough to guarantee the correct propagation of the acoustic pulse in the test piece, Synthetic Aperture Focussing Technique (SAFT) can be applied to improve the image quality by beamforming.

Conventional SAFT

Supossing that we are using a linear array with N elements, SAFT ultrasonic imaging is based on the sequential activation, one by one, of each array element in emission-reception. The adquired data are then organised in the image system memory in order to apply beamforming in a second stage.

To apply the linear array technique, a subset of M signals (where $M < N$) corresponding to M consecutive elements in the aperture can be combined in the beamformer by using suitable delays for dynamic focussing in emission and reception.

Then, the j^{th} A-scan $S_j(z)$, where $(j = 1, \cdots N - M + 1)$, corresponding to the center of the j^{th} subaperture, is composed by:

$$S_j(z) = \sum_{i=j}^{j+M} s_{ii}(t - 2T_i(z)) \tag{1}$$

where M is the subaperture size, $s_{ii}(t)$ is the signal emitted and received by the i^{th} element, where $(i = 1, \cdots N)$, and $T_i(z)$ is the delay necessary to focus at depth z, that is applied twice to compensate the two-way path.

Then, until all the elements of the array are employed this subset is swept, element to element, along the stored signals to produce $N - M + 1$ consecutives A-scans. This step, which defines the distance between two lines in the image, is equal to the array pitch d. Hence, as the lateral resolution is determined by the aperture size, it is possible to link both parameters to determine the optimal value of M thorought the resolution in the image. If $Md >> \lambda$:

$$Resolution = 2z \cdot \arcsin\frac{\lambda}{Md} \approx 2z\frac{\lambda}{Md} = 2d \Rightarrow M \leq z\frac{\lambda}{d^2} \tag{2}$$

where z is the depth position and λ the wavelength.

As the A-scan is obtained in a postprocessing stage, the value of M can be dynamically changed to maintain constant lateral resolution at all depths.

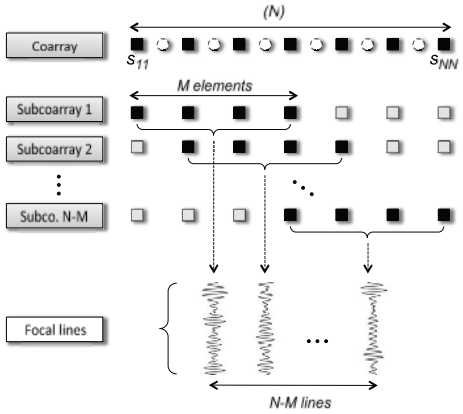

FIGURE 1. Conventional SAFT applied to linear scanning. Each line in the image is composed by the beamforming of the signals of M consecutive elements.

After all A-scan have been obtained, the B-scan image is composed by assembling the $N-M+1$ A-scans obtained. An example for $N=7$ and $M=4$ is presented in figure 1.

The process of A-scan beamforming can be studied by using the concept of coarray, also known as effective aperture, that is used to model the pulse-echo response in continuous wave of an imaging system [4]. In synthetic aperture systems the coarray may be expressed like a sum of several subcoarrays, each one obtained as the convolution of one subaperture in emission and one in reception[3]. Then, the coarray that compose the A-scan with M consecutive elements in the aperture is:

$$w_{SAFT}(n) = \sum_{i=1}^{M} \delta(n-i) * \delta(n-i) \tag{3}$$

where $\delta(n-i)$ is the i^{th} subaperture composed by the i^{th} element. A graphical description is presented in figure 2a.

Considering that the distance between elements is $d > 2\lambda$, the pulse-echo process composes a coarray response with a virtual distance between elements of $2d > 4\lambda$. Then, if the beampattern of the coarray is computed, it can be seen that the A-scan composition can introduce artifacs in the image due to the grating lobe formation (figure 2b). The total beampattern is:

$$|W_{SAFT}(\theta)| = |FFT\{w_{SAFT}\}| = \left| \frac{\sin(kMd\sin\theta)}{\sin(kd\sin\theta)} \left[\frac{\sin(ak/2\sin\theta)}{k/2\sin\theta} \right]^2 \right| \tag{4}$$

where $k = 2\pi/\lambda$.

The first term in the former equation is the array factor of the coarray, and the second term is the diffraction pattern of the element, which has a size of a. The element response, that modulates the diffraction pattern, has been represented in the figure 2b with a dashed line. In this case, where $d = 2\lambda$, grating lobes are produced at 15deg meanwhile the minimum in the element diffraction pattern is produced at 30deg.

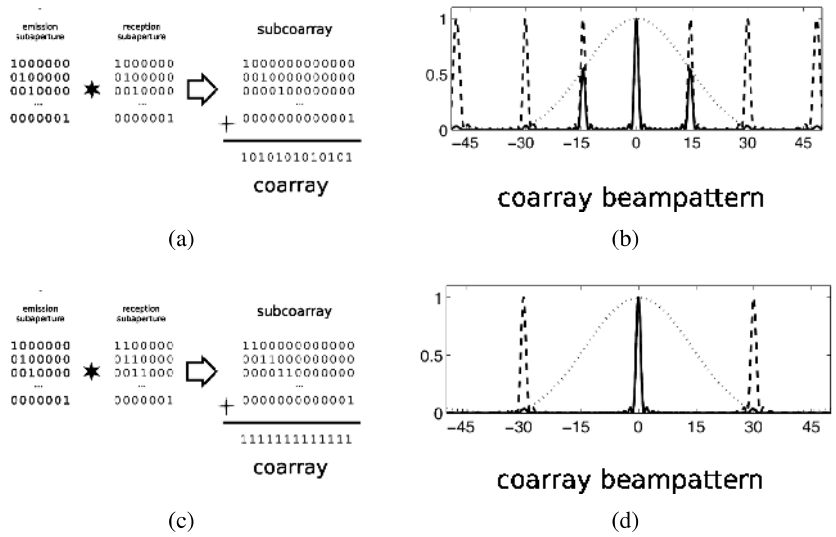

FIGURE 2. For a linear array of $d = 2\lambda$ and $M = 32$, (a) Conventional SAFT coarray composition; (b) Conventional SAFT coarray beampattern; (c) 2R-SAFT coarray composition; (d) 2R-SAFT coarray beampattern.

2R-SAFT

To avoid grating lobe formation a new SAFT technique, known as 2R-SAFT, based on the use of one element in emission and two reception is applied. The ith element of the array operates in pulse-echo whereas the $(i+1)^{th}$ element operates in reception. The last element of the aperture operates in pulse-echo mode only [3]. A graphical description of the process is presented in figure 2c. As it can be seen, the coarray gaps produced in conventional SAFT (figure 2a) are now filled by this second receiver, achieving a distance between elements equivalent to the pitch of the original array. Consequently, a total of $(2N-1)$ signals are obtained, instead of N as in conventional SAFT. Then, the coarray that compose the A-scan with M consecutive elements in the aperture is:

$$w_{2R-SAFT}(n) = \delta(n-M) * \delta(n-M) + \sum_{i=1}^{M-1} \delta(n-i) * (\delta(n-i) + \delta(n+1-i)) \qquad (5)$$

And its beamfoming pattern is modelled by:

$$|W_{2R-SAFT}(\theta)| = |FFT\{w_{2R-SAFT}\}| = \left| \frac{\sin[dk/2(2M-1)\sin\theta]}{\sin(dk/2\sin\theta)} \left[\frac{\sin(ak/2\sin\theta)}{k/2\sin\theta} \right]^2 \right| \qquad (6)$$

As it can be seen in figure 2d, now the grating lobes are located at positions where the element diffracction pattern has a minimum. Then, if the steering is maintaned around the axis, grating lobe formation is avoided.

Now, in order to obtain the corresponding j^{th} A-scan, maintaning the same lateral resolution than in the conventional SAFT case, a subset of $2M-1$ signals, corresponding to M consecutive elements in the aperture, are combined in the beamformer. Due to the number of

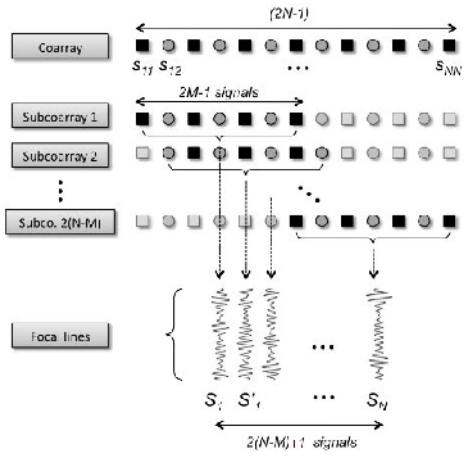

FIGURE 3. 2R-SAFT, each line in the image is composed by the beamforming of the signals of 2*M-1 consecutive signals.

signals respect to the conventional SAFT is doubled, the signal to noise ration in the A-scan is increased. If we take transducer elements as a reference to step-swept along the aperture, the j^{th}, where ($j = 1, \cdots N - M + 1$), A-scan is composed as:

$$S_j(z) = \sum_{i=j}^{j+M-1} s_{ii}(t - 2T_i(z)) + \sum_{i=j}^{j+M-2} s_{i(i+1)}(t - T_i(z) - T_{(i+1)}(z)) \tag{7}$$

where $s_{i(i+1)}$ is the signal emitted by the i^{th} element and received by $(i+1)^{th}$ element, and $T_{(i+1)}(z)$ is the focussing delay of the $(i+1)^{th}$ element at depth z. Then, the obtained B-scan is equivalent in size and resolution with the conventional SAFT.

However, if the step is based on acquired signals instead of elements in the aperture, additional lines $S_{j'}(z)$, where ($j' = 1, \cdots N - M$), can be generated between two consecutive $S_j(z)$ lines.

$$S_{j'}(z) = \sum_{i=j'+1}^{j'+M-1} s_{ii}(t - 2T_i(z)) + \sum_{i=j'}^{j'+M-1} s_{i(i+1)}(t - T_i(z) - T_{(i+1)}(z)) \tag{8}$$

Now, the B-scan image is composed by $2(N-M)+1$ lines with a distance of $d/2$ between them, where $S_j(z)$ are the even lines and $S_{j'}(z)$ the odd lines of the B-scan image (figure 3). This fact allows to increase the lateral resolution, producing a new B-scan image with double of lines and double resolution than the conventional SAFT. Consequently, the optimal subaperture size M will be:

$$M \leq 2z\frac{\lambda}{d^2} \tag{9}$$

RESULTS

To evaluate the performance of the proposed algorithm, results obtained in CFRP components inspection are presented. Composite structures can be damaged under mechanical

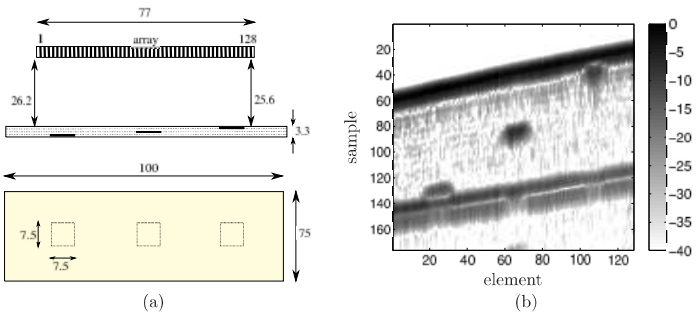

FIGURE 4. (a) Array and CFRP sample (side and top views). Dimensions are in millimeters. (b) Raw B-Scan used to compose SAFT images.

and thermal loadings due to defects ocassioned by the manufacturing process. The typical damage behaviour in the laminated composites is transverse microcracking, fiber-breakage and delamination. Acurate evaluation of their location and morpholgy is necessary in order to determine the correct repair operation [5, 6].

The experiments were conducted in a water tank. The sample was a 3.3 mm thickness laminate of carbon-fiber reinforced plastic (CFRP) composite. In figure 4 a schematic representation of the array and the sample are presented. The array was positioned at about 26 mm from the surface of the sample. Embedded Teflon patches simulate delaminations of 7.5 x 7.5 mm, and they were positioned at three different depths: close to the surfaces and in the middle of the sample.

It was used an immersion-type linear array (Imasonic, France) of 5 MHz center frequency, 128 elements (0.5 mm x 12 mm), 0.6 mm-pitch, which was connected to a commercial equipment (Model SITAU 32:128, Dasel, Spain). Each element of the array was excited with a short pulse (100 ns width, 100 V). The signals were acquired (40 MHz sampling frequency, 12 bits) and stored in the computer for post-processing.

The propagation velocities considered for the calculation of the delays were 1500 $m.s^{-1}$ for water and 2800 $m.s^{-1}$ for the CFRP, and linear interpolation was used to calculate sub-sample contributions. Figure 4b shows a raw B-Scan of a section of the CFRP sample, with dynamic range of 40 dB. The slight tilt of the array with respect to the sample can be clearly observed. On each image it can be clearly seen the top layer, the bottom layer and the three delaminations at different depths.

Figure 5 shows the resulting images obtained with the conventional SAFT (left side) and 2R-SAFT (rigth side) techniques, using Blackman apodization and different sub-aperture sizes (M) of 10, 20 and 40 elements. For comparishon reasons, both techniques use the same value of M. A detail of the intermediate defect is shown in figure 6. The following characteristics can be observed:

- For both configurations, if M increases, the lateral resolution is improved. However, if the detail presented in figure 6 is considered, it can be seen that the achieved improvement in lateral resolution is better for the 2R-SAFT.

- If signal to noise ratio is considered, 2R-SAFT shows better performance than conventional SAFT. In fact, for 2R-SAFT, the signal to noise ratio inside the piece is maintaned constant for all three configurations, whereas it is decreased in the case of conventional SAFT.

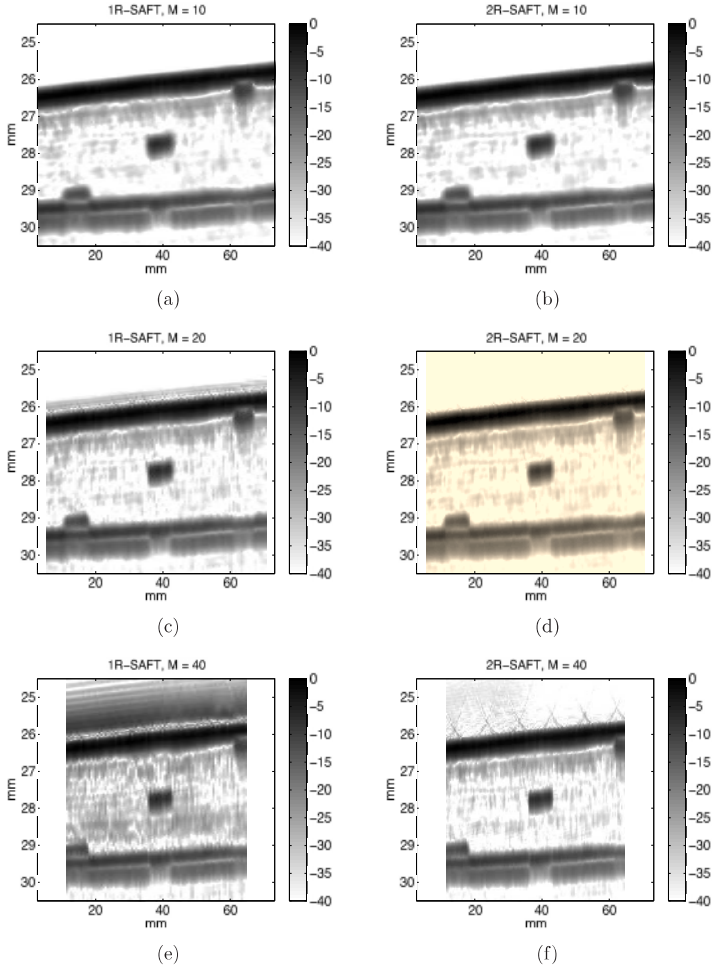

FIGURE 5. B-Scan images for SAFT (left) and 2R-SAFT (right) with different sub-aperture sizes: (top) $M = 10$; (middle) $M = 20$; (bottom) $M = 40$.

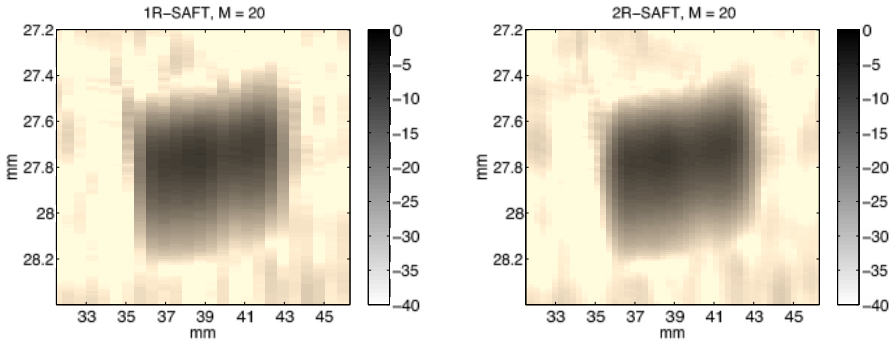

FIGURE 6. With SAFT (left) and 2R-SAFT (right) using $M = 20$ in both cases.

In general it can be concluded that 2R-SAFT improves image quality by increasing M, producing better results than conventional SAFT. However, if M is increased, the image width is reduced and noise is increased for conventional SAFT. By comparing the images, a good compromise choice would be $M = 20$ for both methods.

CONCLUSIONS

A new synthetic aperture beamforming method applied to linear array scanning that uses one element in transmission and two in reception has been presented. This method, known as 2R-SAFT, is based on the coarray configuration and allows dynamic tuning of the beamforming process. Compared with conventional SAFT, this method provides better results due to:

- It avoids grating lobe formation, reducing artifacs in the image.
- It doubles the number of signals that compose each image line, increasing the signal to noise ratio.
- It doubles the number of lines in the image, increasing lateral resolution.

And finally, as the hardware complexity is still very reduced when compared to full phased-array systems, it can be suitable for implementation in embedded or portable systems.

ACKNOWLEDGMENTS

This work was supported in part by the Spanish Ministry of Science and Innovation under Grant BES-2005-7704, BES-2008-008675 and the projects DPI2007-65408-C02-01 and TRA2007-67711/AUT. and R. T. Higuti is at IAI-CSIC as a postdoctoral fellow supported by Brazilian Ministry of Education/CAPES (grant BEX 3711-08-0).

REFERENCES

1. C. Holmes, B. W. Drinkwater and P. D. Wilcox *Ultrasonics* **48**, 636–642 (2008)
2. J. A. Jensen and S. I. Nikolov and K. L. Gammelmark and M. H. Pedersen *Ultrasonics* **44**, 5–15 (2006)
3. C. J. Martín, O. Martínez, L. G. Ullate, A. Octavio and G. Godoy "Reduction of grating lobes in SAFT images" *Proceedings of the 2008 IEEE International Ultrasonics Symposium* edited by IEEE, 2008, pp. 721–724.
4. R. T. Hoctor and S. A. Kassam *Proceedings of the IEEE* **78**, 735–752 (1990)
5. C. Engstrand and R. Kline "Application of SAFT to layered, anisotropic media" in *Review of Progress in Quantitative Nondestructive Evaluation* edited by D. O. Thompson and D. E. Chimenti AIP Conference Processdings vol. 760 American Institute of Physics Melville, NY, 2005, pp.1151–1158.
6. S. C. Wooh and C. Wei *Composites Part B: Engineering* **30**, 433–441 (1999)